Vortex lock-on phenomena due to pulsating flow in tube arrays

by

E. Konstantinidis, D. Castiglia, G. Papadakis, S. Balabani and G. Bergeles[†]

Experimental and Computational Laboratory for the Analysis of Turbulence

Department of Mechanical Engineering, King's College London, Strand, WC2R 2LS, U.K.

[†]Laboratory of Aerodynamics

National Technical University of Athens, Zografou Campus, Athens 157 10, Greece

ABSTRACT

This paper describes an experimental and numerical investigation on the effects of imposed pulsations on the cross-flow over tube arrays in the subcritical regime. Three different arrays were considered, namely inline, staggered and asymmetric with the same streamwise and transverse spacing-to-diameter ratios of 2.1 and 3.6 respectively. A laser-Doppler anemometer was employed for velocity measurements and laser-sheet visualisation was used to reveal the underlying unsteady flow patterns. Simulation of the flow was carried out by solving the Navier-Stokes equations on an orthogonal curvilinear grid and using the Smagorinsky model for scales smaller than the grid size. The time-dependent simulation was performed in two dimensions in order to constrain the computational time while providing data for the entire flow field.

Spectral analysis of the time-resolved velocity data showed that the flow exhibits periodic phenomena that depend strongly on the tube arrangement. Visualisation of the flow indicated that these phenomena are associated with vortex shedding. The observed Strouhal numbers (St) were 0.14 for the in-line and 0.24 and 0.33 for the staggered arrays, whereas for the asymmetric array it was not possible to ascertain a specific value as the shedding period displayed random fluctuations. Pulsing the flow resulted in vortex shedding lock-on. When the non-dimensional pulsation frequency (F) was near twice the unforced Strouhal number, shedding occurred at the sub-harmonic of the pulsation frequency, i.e. St = 0.5F. A second mode of lock-on was observed when F was near the unforced St with St = F. Modification of the vortex shedding characteristics due to lock-on resulted in changes of the time-mean velocity and turbulence characteristics. The amplitude of velocity fluctuations increased with lock-on due to an increase in the amplitude of the organised velocity fluctuations associated with vortex shedding. Numerical predictions were compared with experimental data for the in-line and asymmetric arrays and despite some discrepancies, the results showed better agreement than simulations with standard turbulence models for this complex flow. The effects of imposed pulsation on the velocity characteristics were similar as in the experiment. However, the 2-D simulation of the flow imposes a severe constraint; the effects of the three-dimensional mechanism for the dissipation of vorticity and turbulence production cannot be accounted for in the simulations.

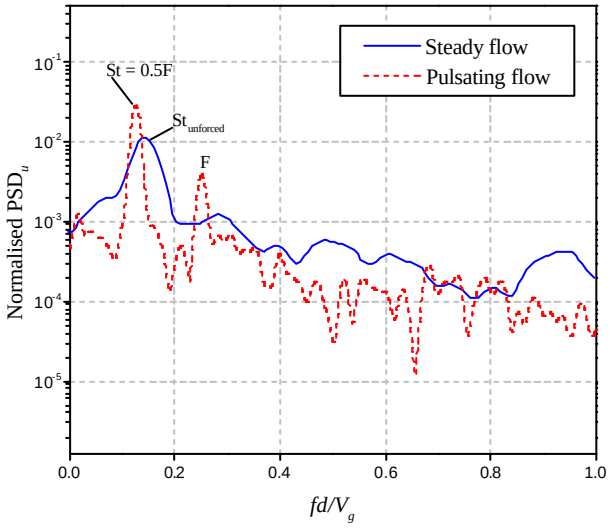

Figure: Typical lock-on of the vortex shedding from a cylinder in the fifth row of an in-line array at the sub-harmonic pulsation frequency.

1 INTRODUCTION

The cross-flow over tube arrays (or banks) continues to attract interest due to its importance in the design of heat exchangers as well as the fact that this complex flow represents a challenging problem for computational fluid dynamics (CFD). There is a marked activity in heat transfer augmentation using various methods, such as modification of the tube surface (e.g. finned or rough or otherwise extended surfaces), of the tube arrangement (e.g. asymmetric), or even of the flow (e.g. superposition of sound on air flows) and a need for relevant experimental data arises. Numerical predictions of the flow normal to banks of tubes with standard turbulence models using Reynolds-averaged Navier-Stokes equations (RANS) has been formidable for high Reynolds numbers. On the other hand, Large Eddy Simulation (LES) codes appear more appropriate for this type of flow (Laurence and Rollet–Miet 1998). However, before LES can be used as a design tool, extensive validation against experimental data must be carried out.

The existence of high levels of turbulence and flow reversals in tube arrays favours the use of Laser Doppler Anemometry (LDA) in order to obtain accurate velocity statistics compared to hot-wire probes. Numerous studies have been presented in previous international LDA symposia providing detailed mappings of the velocity field (Halim and Turner 1986; Simonin and Barcouda 1986; 1988; Balabani et al 1994; Meyer and Larsen 1994; Balabani and Yianneskis 1996). However, most of these studies were limited to time-averaged properties but it is known that the flow in tube arrays exhibits strong periodic phenomena. Balabani and Yianneskis (1996) showed that turbulence levels were overestimated up to 50 % by ensemble averaging due to the variation of the mean flow associated with shear layer instability. Time-dependent heat and mass transfer in tube arrays have also been studied. Nishimura et al (1993) found that both the shear stress and mass transfer exhibit fluctuations at the vortex shedding frequency in a staggered and in an in-line array. Scholten et al (1998) developed a method for the simultaneous acquisition of the unsteady velocity and surface heat flux for tubes in cross-flow that demonstrated the strong dependence of heat transfer on local (temporal) fluid dynamics.

A great deal of understanding of the unsteady phenomena has been achieved by studies of the excitation mechanisms that lead to flow-induced vibrations in heat exchangers. The fluid-excitation mechanisms have been identified and classified as reviewed by Weaver and Fitzpatrick (1988). The existence of discrete periodic phenomena in tube arrays has been recently associated with periodic vortex (or vorticity) shedding by flow visualisation studies (e.g. Price et al 1995; Polak and Weaver 1995; Oengören and Ziada 1998). It has been recognised that vortex shedding induces fluctuating forces on the tubes that, if resonance with a structural or an acoustic frequency occurs, may excite vibrations in liquid flows or noise in gas flows.

Resonance of the vortex and vibration frequencies, usually termed lock-on, can lead to equipment failure, and it often has (Paidoussis 1983). However, it appears that the flow under resonance conditions is more active and heat transfer rates are higher than at off-resonance. For instance, Base et al (1981) found a considerable increase in heat transfer of a vibrating heat exchanger. Credence to the rather rudimentary experiments of Base et al (1981) has been provided from studies of heat transfer measurements around a transversely oscillating cylinder (Cheng et al 1997; Gau et al 1999). These studies demonstrated quite clearly that there is an increase in heat transfer associated with lock-on. Vortex lock-on has also been observed when the cylinder oscillates in-line with the flow direction or when the flow contains a periodic component superimposed on the mean flow and the cylinder is stationary (Barbi et al 1986; Griffin and Hall 1991). The latter type of flow is commonly termed pulsating flow and this terminology is adopted here. Evidence from mass transfer measurements around a cylinder in pulsating cross-flow also suggest that transfer rates increase with lock-on (Sung et al 1994). Therefore, it can be argued that pulsating flow offers a potential method for heat transfer augmentation in heat exchangers.

The present study forms part of a systematic effort to examine the flow and heat transfer characteristics in tube arrays with the objective to improve the efficiency of heat exchangers. This paper provides an account of the most important findings of this ongoing investigation up to this point. The flow in three tube arrays was investigated experimentally by means of LDA measurements and flow visualisation. The streamwise and transverse spacing to diameter ratios were the same for all arrays but the arrangement of the tubes was different forming in-line, staggered and asymmetric arrays. In addition to the influence of the arrangement of the tubes on the flow, the effect of pulsation is examined for each array. Concurrently, numerical predictions are presented and compared with the experimental data.

2 EXPERIMENTS

2.1 Test models

The three tube arrays studied are shown in figure 1. They comprise in-line, staggered and asymmetric arrays with the same streamwise and transverse spacing of 21 mm and 36 mm respectively. The asymmetric and staggered arrays

can be produced from the in-line array by displacing the tubes of the odd-numbered rows by 18 mm and -10 mm respectively in the transverse direction. The tubes were circular cylinders, 10 mm in diameter. The models were fitted across the 72-mm square test section and half tubes were mounted on the test section walls to simulate an infinite array and minimise wall effects. The tubes were rigidly mounted on the walls to eliminate vibrations. The test section was made of acrylic plastic to allow optical access and the cylinders were of the same material. The in-line and staggered arrays are scale models of typical heat exchanger geometries of lignite utility boilers used in the power generation industry, whereas the asymmetric array was used in order to examine the influence of tube arrangement. The selection of the scale-down factor was based on a compromise between resolving the interstitial flow adequately while maintaining sufficient number of tubes in the model.

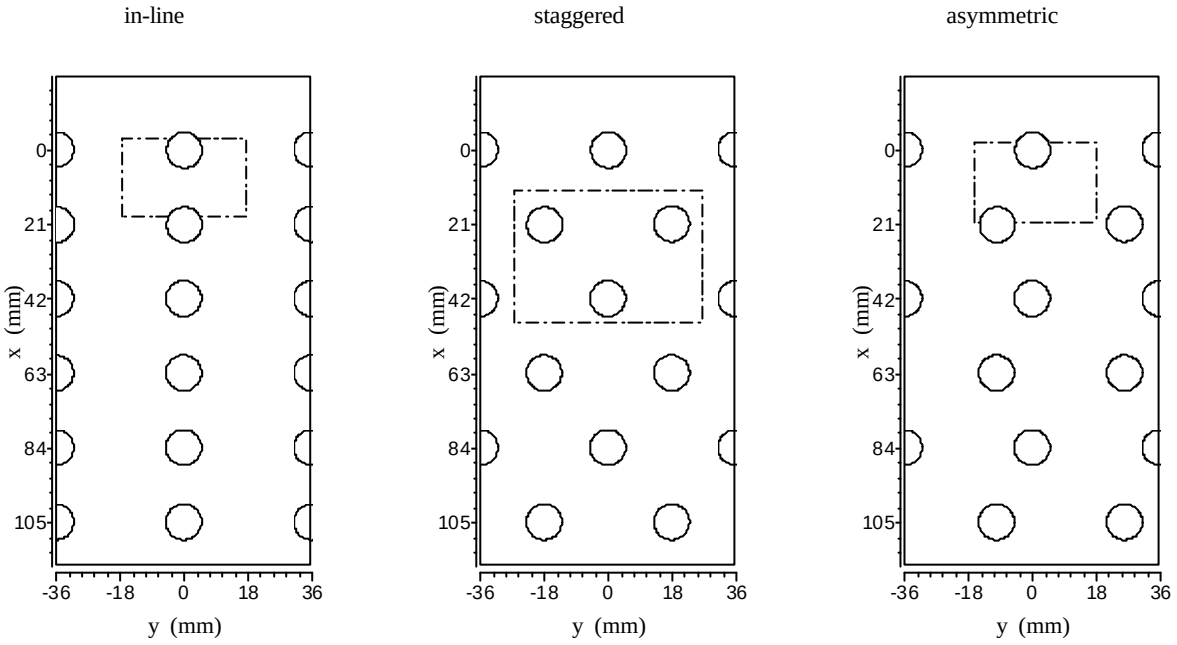

Figure 1. Schematic cross-section of the tube arrays used in the present investigation. Flow direction is from top to bottom and the origin of the coordinate system is positioned at the centre of the middle cylinder of the first row. Dash-dotted rectangles delineate the area of the flow shown in the visualisation pictures in figure 3.

2.2 Water tunnel

The experiments were conducted in a purpose-designed closed-circuit water tunnel (Balabani et al 1994; Balabani and Yianneskis 1996) modified to produce pulsating flow. The flow in the tunnel was driven by a centrifugal pump delivering flow velocities up to 0.95ms^{-1} adjustable by a bypass valve. A bifurcation in the circuit divided the flow into two branches and a rotating valve periodically blocked the flow passage of one branch, thereby producing periodic unsteadiness with a profile similar to a sinusoidal pulsation. The frequency of the pulsation was adjusted by the speed of the rotating valve via a variable speed motor. Control valves adjusted the relative amounts of steady/pulsed flow. With the present experimental set-up, the mean flow-rate, the frequency and the amplitude of the pulsation could be adjusted independently and in continuous increments.

The upstream flow velocity was measured with a variable area rotameter in steady flow. In pulsating flow the upstream velocity was monitored by measuring the velocity at a reference point using the Laser Doppler Anemometer described below. The flow velocity was estimated from the mean velocity at the reference point, which was calibrated against the rotameter readings in steady flow. The frequency of pulsation was monitored via an optical encoder attached to the shaft of the rotating valve and verified by the auto-spectrum of the velocity, whereas the amplitude of the pulsation is calculated by the variation of the mean velocity at the reference point. The upstream flow had a fully developed turbulent profile, which was not affected by flow pulsation. In this study, the gap velocity, Vg, i.e. the mean flow velocity at the minimum transverse gap between the tubes, and the cylinder diameter, d, are used in the definitions of Reynolds number, $\mathrm{Re} = V_g d / n$, non-dimensional pulsation frequency, $\mathrm{F} = f_p d / V_g$,

and Strouhal number, $St = f_S d / V_g$ where f_P and f_S are the frequencies of pulsation and vortex shedding respectively. The experimental uncertainty in determining Re and F is less than 3 %.

2.3 Measurement techniques

A dual beam Laser Doppler Anemometer (LDA) with a 10 mW He-Ne laser source operating in forward scatter was employed for the velocity measurements. The control volume of the intersecting beams was 48.8 μm in diameter and 466 μm in length. A photomultiplier collected the scattered light from particles crossing the control volume and the produced signal was processed using a TSI frequency counter, model 1990B, interfaced to a computer with appropriate data acquisition software. Measured ensemble-averaged mean and r.m.s. velocities are accurate to within 5 and 10 percent respectively. The uncertainty is expected to be higher due to positional errors, especially in regions of steep gradients. Time-resolved velocity data were stored on the computer for subsequent analysis. The raw data were re-sampled at equal time intervals using a linear interpolation and spectra were obtained by the fast Fourier transform method.

In order to visualise the interstitial flow between the tubes, the flow was seeded with 0.015-mm hollow glass particles and a Argon-laser sheet illuminated the test section at right angles to the axes of the tubes and midway the test section. Because of the half tubes on the side-walls, the interstitial flow could be illuminated only with light passing through the cylinders and thus lighting was not homogeneous, producing light and dark patches. The glass particles were neutrally buoyant and followed the flow faithfully. Video recordings of the flow were taken using a CCD video camera with a zoom lens and individual frames of the video were obtained by digitising the video frames with a video grabber.

2.4 Numerical method

A time-dependent simulation using a sub-grid scale model in the context of LES is performed in two-dimensions for the flow in the in-line and asymmetric arrays. The numerical method is similar to that of Bouris and Bergeles (1999) and is based on the solution of the volume averaged Navier-Stokes equations (according to Schumann 1975) on an orthogonal curvilinear grid. The resulting equations have the following general conservative form:

$$\frac{\partial}{\partial t}(r\Phi)+\frac{1}{l_x l_h}\frac{\partial}{\partial x}(r u_x l_h \Phi)+\frac{1}{l_x l_h}\frac{\partial}{\partial h}(r v_h l_x \Phi)-\frac{1}{l_x l_h}\frac{\partial}{\partial x}(m_{eff}\frac{l_h}{l_x}\frac{\partial \Phi}{\partial x})-\frac{1}{l_x l_h}\frac{\partial}{\partial h}(m_{eff}\frac{l_x}{l_h}\frac{\partial \Phi}{\partial h})=S_\Phi \qquad (1)$$

where l_x and l_h are the spatially varying metric coefficients related to the orthogonal curvilinear coordinates (x,h) and S_Φ is the source term. For $\Phi = 1, u_x, v_h$ the continuity and the momentum equations are obtained respectively. It should be pointed out that velocities u_x, v_h are always defined as being normal to the grid lines of constant x,h respectively. The source term involves large but well-known expressions in computational fluid dynamics and is not presented here due to lack of space but it can be found in Mouzakis and Bergeles (1991). The effective viscosity is given by the formula $m_{eff} = m + m_t$ where m_t is calculated for the sub-grid scale fluctuations according to the model of Smagorinsky (1963) and Lilly (1967):

$$m_t = r(C_s\Delta)^2\left|\overline{S}\right| = r(C_s\Delta)^2(2\overline{S}_{i,j}\overline{S}_{i,j})^{1/2} \quad i,j = x,h \qquad (2)$$

$$\overline{S}_{xx} = 2\left(\frac{1}{l_x}\frac{\partial u}{\partial x}+\frac{v}{l_x l_h}\frac{\partial l_x}{\partial h}\right), \quad \overline{S}_{hh} = 2\left(\frac{1}{l_h}\frac{\partial v}{\partial h}+\frac{u}{l_x l_h}\frac{\partial l_h}{\partial x}\right)$$

$$\overline{S}_{xh} = \frac{1}{l_x}\frac{\partial v}{\partial x}+\frac{1}{l_h}\frac{\partial u}{\partial h}-\frac{v}{l_x l_h}\frac{\partial l_h}{\partial x}-\frac{u}{l_x l_h}\frac{\partial l_x}{\partial h} \qquad (3)$$

where Δ is the filter width, defined as $\Delta = (\Delta x \cdot \Delta h)^{0.5}$ and C_S is a constant equal to 0·1. Velocities are stored at the centre of the computational cells and the original SIMPLE algorithm (Patankar and Spalding 1972) is used to deal with the pressure coupling of the momentum and continuity equations. In order to avoid the checkerboard pressure field, the method proposed by Rhie and Chow (1983) was employed.

A fully implicit method was used for the solution of the above equations i.e. the momentum, continuity and energy equations converged at each time step prior to proceeding to the next one. For the computation of the temporal term, a first order Euler discretisation was employed. For the discretisation of the diffusion terms the central difference

scheme was used and for the convection terms a higher order bounded scheme was used developed by Papadakis and Bergeles (1995).

3 RESULTS AND DISCUSSION

3.1 Overview of vortex shedding in steady flow

Typical auto-spectra of the streamwise velocity fluctuations in the three tube arrays for steady flow are shown in figure 2. The in-line array exhibits a discrete frequency with a Strouhal number of 0.14 (figure 2a). Detailed results for the in-line array can be found in Konstantinidis et al (2000). Measurements at different locations and at different Reynolds numbers produced the same Strouhal number with the exception of the flow in the gap between the first and second row tubes. It was found that the tube in the second row shielded the shear layers separating from the tube in the first row and the flow in the gap between them resembled a cavity flow. The observed Strouhal number is in agreement with results obtained in in-line arrangements with similar streamwise spacing (Weaver et al 1987). The staggered array exhibits two discrete frequencies (figure 2b) with Strouhal numbers of 0.24 and 0.33. It is known (Oengören and Ziada 1998) that some staggered arrays exhibit double frequencies and this is the case here. As with the in-line arrangement, measurements at different locations and at different Reynolds numbers yielded the same Strouhal numbers. The location where each peak appears and disappears suggested that the high frequency is caused by vortex shedding from the front rows whereas the low frequency stems from shedding from the inner rows. Although direct comparison with other data in the literature is not possible, the results agree fairly well with results obtained in rotated square arrays with similar pitch to diameter ratio to the one used in the present study (Weaver et al 1987). In contrast to the discrete frequencies observed in the in-line and staggered arrays, the spectrum of the velocity fluctuations in the asymmetric array exhibits a broad band of frequencies (figure 2c). It was not possible to ascertain a Strouhal number by measurements at different locations and different Reynolds numbers for the asymmetric array, although some measurements indicated more discrete peaks. However, the broadband seen in the spectrum in figure 3c extended to higher frequencies as the Reynolds number was increased. Therefore, a similar phenomenon to the constant Strouhal number one exists in the asymmetric array but is not as discrete as in the in-line and staggered arrays.

Figure 3 shows visualisation pictures of the interstitial flow in the three arrays illustrating coherent vortices. Video playback of the flow showed clearly that vortex shedding occurs in the three arrays. Based on the flow visualisation experiments, the period associated with the shedding phenomena could be determined within ±0.02s. For the in-line array, the Strouhal number was consistent with that found through the LDA measurements and was the same for all rows. For the staggered array, the period of vortex shedding found was consistent with the low Strouhal number, and could be measured only for rows 3 to5. For the first and second row, the vortex shedding process was not well defined and the period could not be determined. For the asymmetric array, no repeatable period of any pattern could be identified although vortex shedding was evident. The asymmetry of the geometry imposes a distorted wake that affects the vortex shedding mechanism. It can be argued that there is an element of randomness inherent in the process and that vortex shedding is sensitive to temporal and local instabilities of the flow in the asymmetric array.

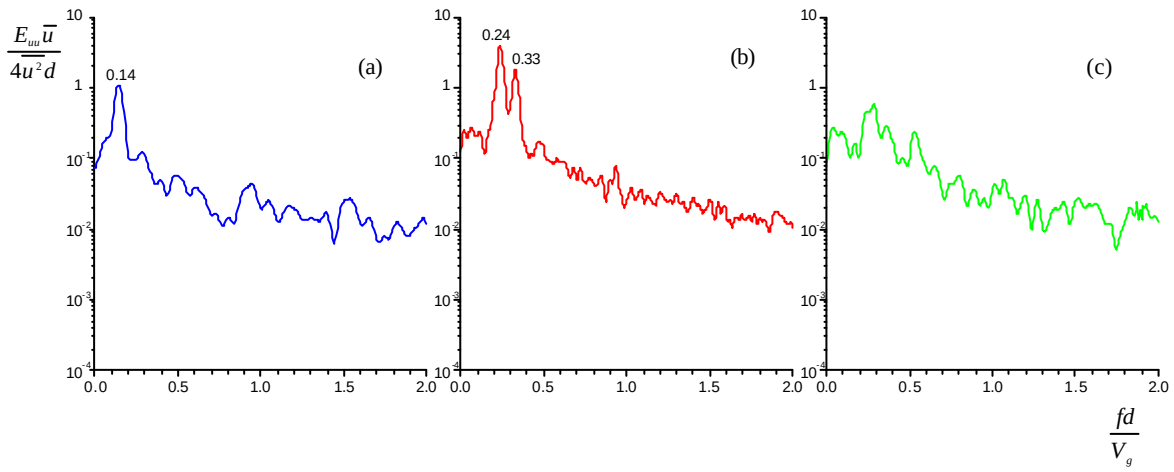

Figure 2. Normalised auto-spectra of the streamwise velocity fluctuations for steady flow.
(a) In-line, Re = 2800, measured at x/d = 5.4, y/d = 0.5.
(b) Staggered, Re = 7100, measured at x/d = 4.2, y/d = 0.9.
(c) Asymmetric, Re = 3500, measured at x/d = 5.2, y/d = 0.5.

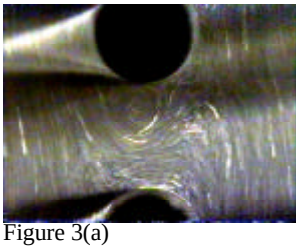

Figure 3(a)

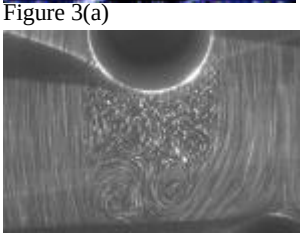

Figure 3(c)

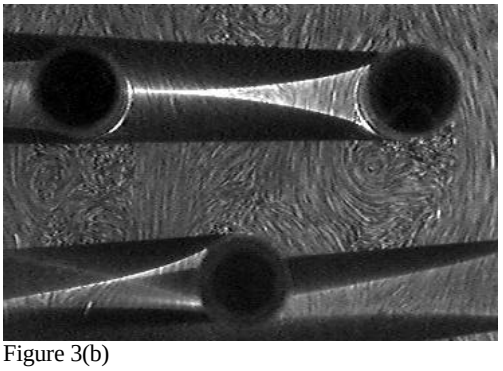

Figure 3(b)

Figure 3. Flow visualisation pictures illustrating coherent vortices (steady flow) in the wakes of the tubes in the areas shown in figure 1; (a) in-line, Re = 3500, (b) staggered, Re = 1400 and (c) asymmetric array, Re = 1100.

3.2 Effect of pulsating flow on vortex shedding

In consideration of the lock-on phenomenon observed in pulsating flow over a single cylinder, two questions arise with regard to pulsating flow over tube arrays: (1) will lock-on of the pulsation and vortex shedding frequencies occur in tube arrays and (2) if it does, what would be the relevant ranges of the non-dimensional frequency, $F = f_p d / V_g$, and the non-dimensional amplitude, $e = \Delta U / (2\pi f_p d)$, for lock-on since tube arrays have different Strouhal numbers (generally much higher) than a single cylinder. The experimental results showed that lock-on occurs in all three arrays investigated and two different modes of lock-on were identified. Detailed experiments were carried out only in the staggered array. The results (to be published) were obtained over a wide range of non-dimensional frequencies (F) indicated that there is a range of F values for which lock-on occurs, similar to that for a single cylinder. When the frequency of pulsation is roughly twice the frequency of unforced vortex shedding then vortex shedding is forced at the sub-harmonic of the pulsation frequency. Generally, in all three arrays the wake of the tubes in the first row was easily locked on half the pulsation frequency. This effect, however, was less strong in the inner rows having a tendency to weaken with row depth. Notwithstanding the diminishing effects of pulsation with row depth, it was found that for certain conditions vortex shedding from all rows in the array was locked on half the pulsation frequency. The second mode of lock-on was observed when the pulsation frequency was near the unforced vortex shedding frequency; then shedding was forced at the pulsation frequency. This mode was observed only for pulsation frequencies very close to the unforced vortex shedding frequency, the resonance was less intense compared to the sub-harmonic lock-on and occurred primarily in the first row for the in-line and staggered arrays. Interestingly, for the asymmetric array the second mode of lock-on persisted up to the fifth row with the last row exhibiting the sub-harmonic lock-on. The effect of the non-dimensional amplitude, e, is as important as the non-dimensional frequency, F. The higher e, the wider the lock-on range in terms of F is and lock-on is sustained deeper in the array.

Figure 4 shows normalised auto-spectra of the streamwise velocity fluctuations, for such conditions that sub-harmonic lock-on occurs throughout the array. Therefore, the shedding frequency peak occurs at the sub-harmonic of the pulsation frequency, i.e. St = 0.5F. Apparently, a peak is also present at the pulsation frequency, F. In the spectra of figure 4c numerous harmonics of the vortex shedding frequency are present. This is due to the fact that the variation of the flow at the shedding frequency is not exactly sinusoidal and it is a characteristic of the phase-locking of the pulsation and shedding frequencies. Similar results have been observed by other investigators for a single cylinder in pulsating cross-flow (Telionis et al 1993). The shift of the vortex shedding frequency from the unforced Strouhal number to half the non-dimensional pulsation frequency can be readily verified by comparison with the spectra in figure 2. Common features in the three arrays are that the spectral peaks due to vortex shedding are clearer, the height increased and the width reduced compared to the steady flow spectra. These results suggest a well-organised periodic motion of the flow field at a sharply defined frequency. A question that remains is whether the evident changes in the spectral characteristics are accompanied by analogous changes of the velocity characteristics. The succeeding section addresses this issue.

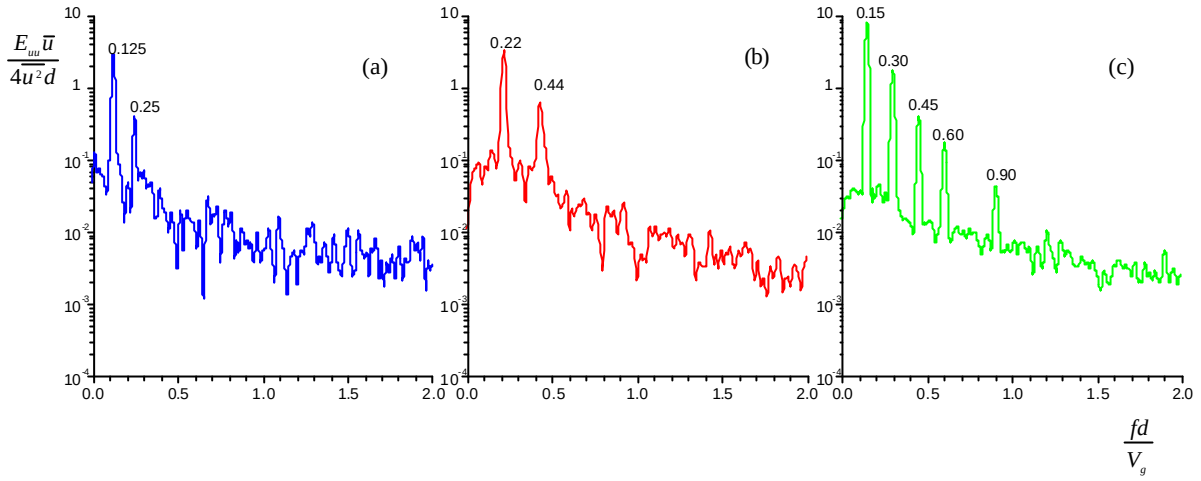

Figure 4. Normalised auto-spectra of the streamwise velocity fluctuations for pulsating flow.
(a) In-line, Re = 2800, F = 0.25, e = 0.13, measured at x/d = 5.4, y/d = 0.5.
(b) Staggered, Re = 2300, F = 0.44, e = 0.05, measured at x/d = 5.4, y/d = 0.5.
(c) Asymmetric, Re = 3500, F = 0.30, e = 0.10, measured at x/d = 5.2, y/d = 0.5.

3.3 Lock-on effect on mean velocity and turbulence

The mean and r.m.s velocity profiles obtained in steady and pulsating cross-flow are compared in figures 5, 6 and 7 for the in-line, staggered and asymmetric tube array respectively. Figures 5 and 7 also contain numerical predictions of the profiles. The flow conditions and the vortex shedding characteristics are given in the associated captions. The velocity data have been normalised with the flow velocity upstream of the bank, U_o. The root mean square value of the velocity fluctuations is presented in terms of $u^*_{r.m.s.} = \sqrt{u^2_{r.m.s.} - u^2_{r.m.s.upstream}}$ in order to facilitate comparison of the experimental data with the numerical predictions because of different upstream turbulence levels. This data reduction also allows comparisons to be made between the steady and pulsating flow data since the apparent increase in r.m.s velocities due to pulsation is removed. For the in-line and staggered arrays LDA measurements were confined to $0 = y/d = 1.8$ as the flow was found to be symmetric with respect to the y-axis. For the asymmetric array LDA measurements covered the range $-2.0 = y/d = 2.0$. In the numerical predictions the entire flow field of each array was modelled as appears in figure 1. The computational mesh consisted of 505×181 cells for the in-line and 632×267 cells for the asymmetric array. A detailed analysis of the presented results is not possible in the space available. Generally, it can be seen that lock-on resulted in changes in the structure of the wakes. The r.m.s. velocity fluctuations appear higher in pulsating flow. Such increases were found to be associated mainly with increases of the velocity fluctuations at the vortex shedding frequency as it is also indicated by the spectral characteristics. Therefore, the r.m.s. velocity is considerably higher behind the tubes of the first row in each array where the lock-on effect was more pronounced. In inner rows, the difference between steady and pulsating flow becomes smaller.

The numerical predictions are reasonably close to the experimental values. The trends of the mean velocity are correctly predicted in terms of the effect of flow pulsation. The r.m.s. velocities are over-predicted and there exist some discrepancies between the experimental and predicted trends. Nonetheless, the predictions with the present model are significantly closer to the experiment compared with RANS turbulence models (Simonin and Barcouda 1988; Balabani et al 1994; Meyer and Larsen 1996). It must be stressed that predictions were made over the entire experimental flow field and this limits substantially the available resources especially in terms of grid refinement. However, this approach does not require any ad-hoc boundary conditions to be determined by experiments. In view of the above, the numerical approach used produced very encouraging results. The main drawback of the present approach was the limitation of the simulation in two dimensions, which is addressed below.

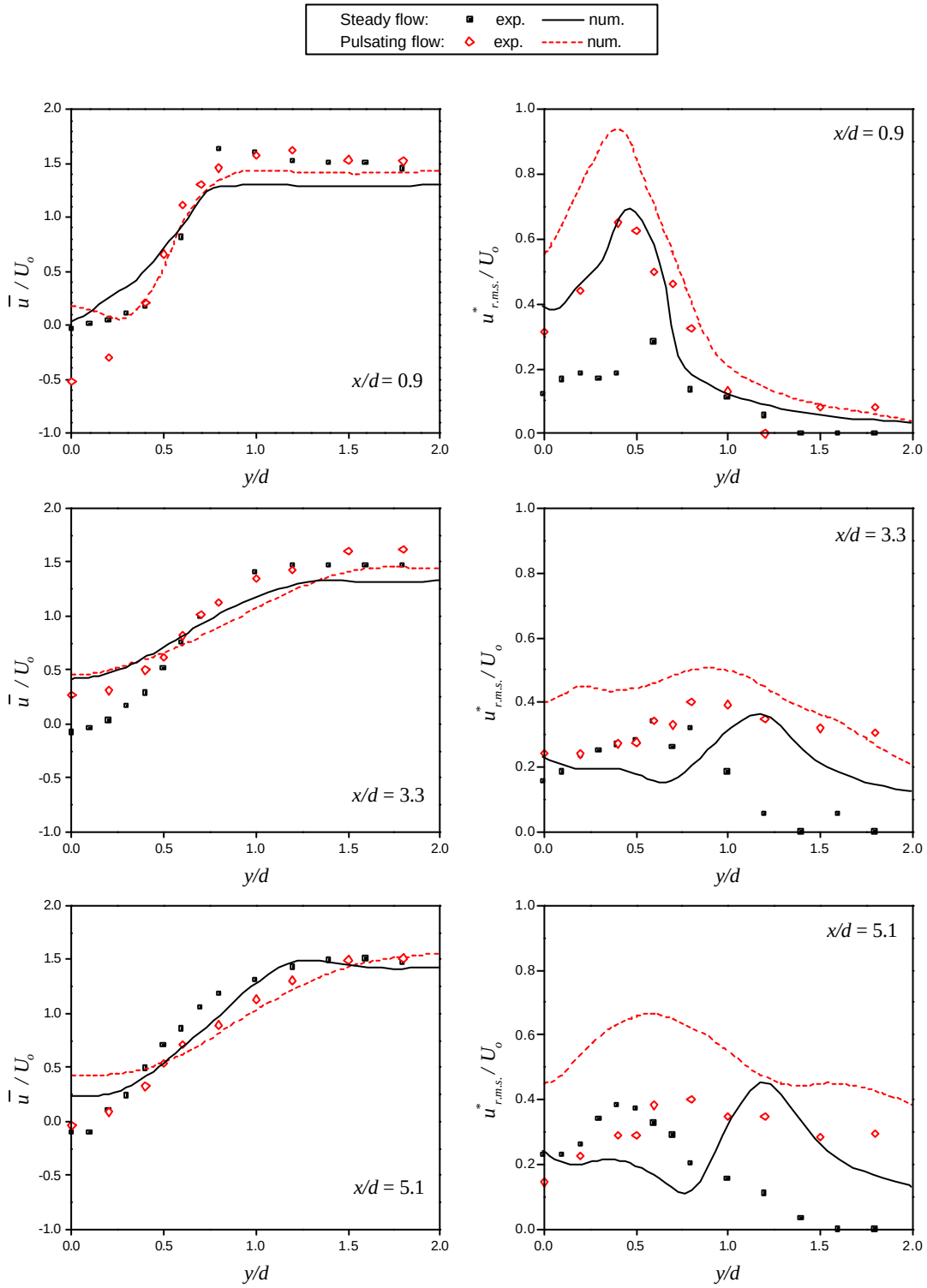

Figure 5. Comparison of the mean and r.m.s. velocity profiles between steady and pulsating cross-flow for three different stations in the in-line array. Symbols represent experimental results and lines numerical predictions.
Experiments - steady flow: Re = 3000, St = 0.14; pulsating flow: Re = 3000, F = 0.3, e = 0.07, St = 0.15.
Numerical - steady flow: Re = 3400, St = 0.15; pulsating flow: Re = 4200, F = 0.24, e = 0.09, St = 0.12.

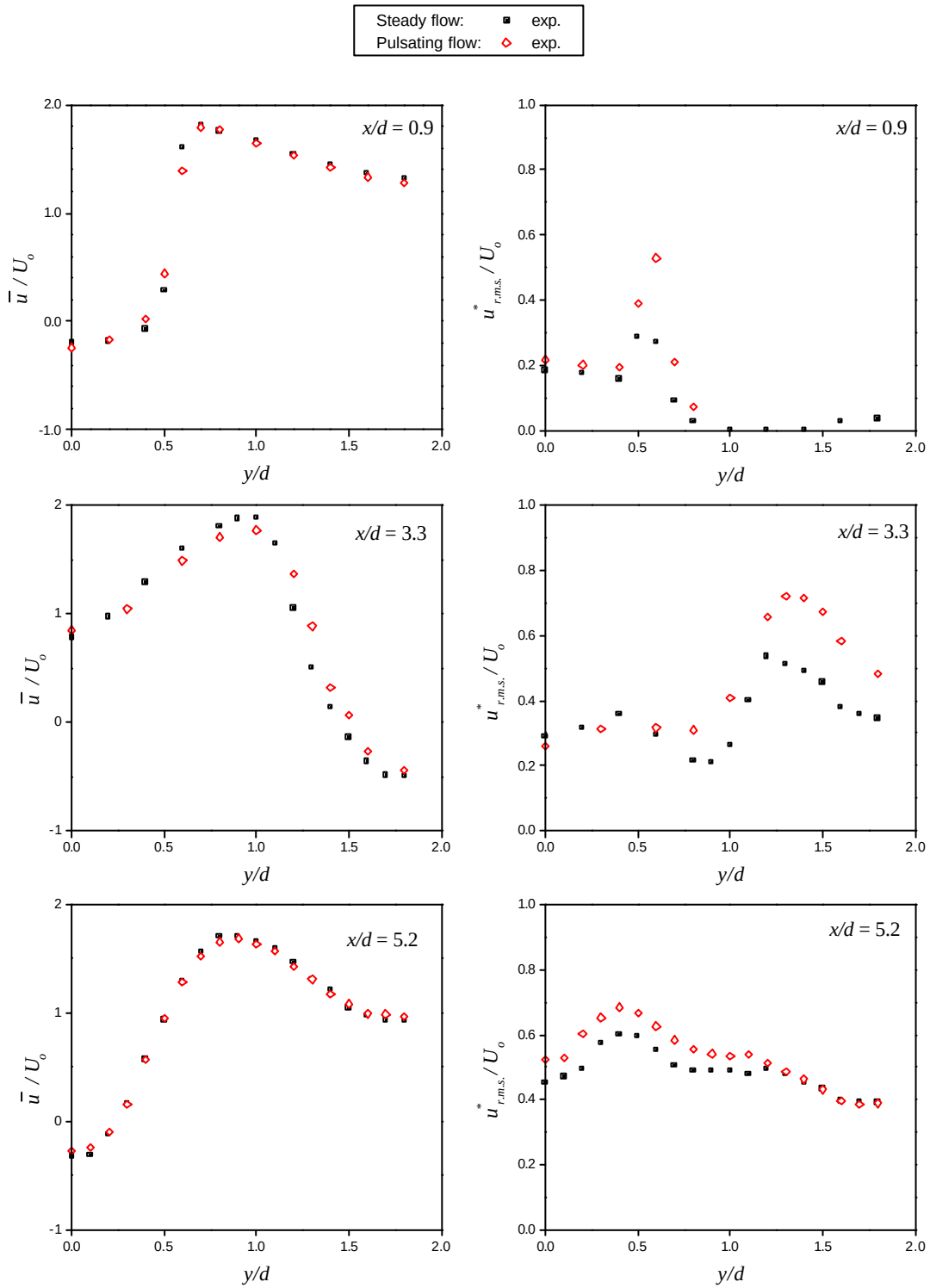

Figure 6. Comparison of experimental mean and r.m.s. velocity profiles between steady and pulsating cross-flow for three different stations in the staggered array. Steady flow: Re = 5900, St = 0.24 and 0.33; pulsating flow: Re = 5800, F = 0.17, e = 0.07, St = 0.17 (lock-on only for the first row).

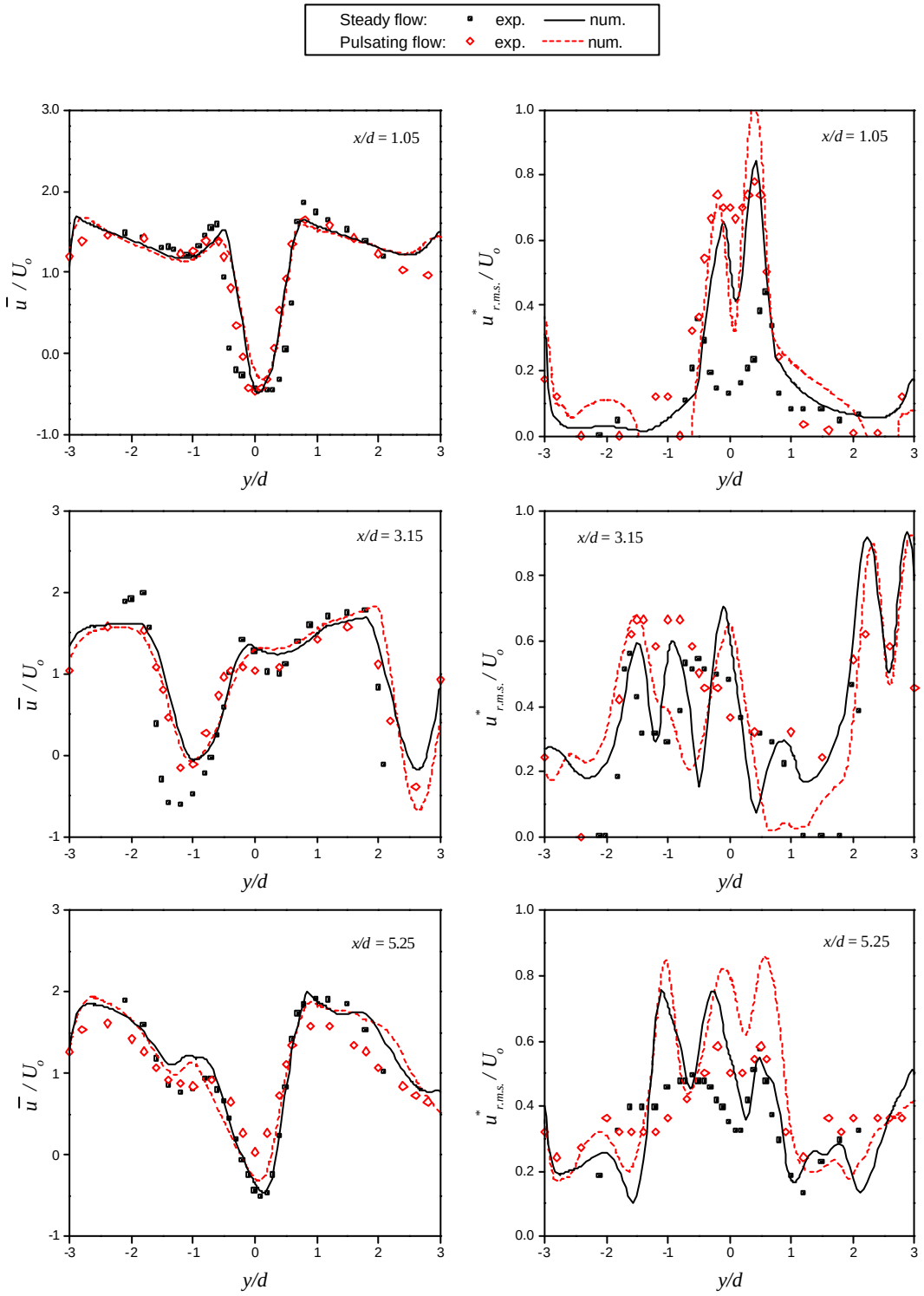

Figure 7. Comparison of the mean and r.m.s. velocity profiles between steady and pulsating cross-flow for three different stations in the asymmetric array. Symbols represent experimental results and lines numerical predictions.
Experiments - steady flow: Re = 3500, St = (not determined); pulsating flow: Re = 3500, F = 0.28, e = 0.09, St = 0.28.
Numerical - steady flow: Re = 5100, St = 0.23; pulsating flow: Re = 5100, F = 0.21, e = 0.12, St = 0.21.

3.4 Three-dimensionality and turbulence

The flow in the three tube arrays used in the present experiments was found to be two-dimensional, i.e. the mean velocity in the direction parallel to the axis of the tubes was approximately zero. The instantaneous flow, however, exhibited strong three-dimensional phenomena, most noticeably, the production of streamwise vorticity. It was observed that the initially 2-D coherent vortices shown in figure 3 dissipated rapidly into 3-D turbulence downstream, probably under the action of vortex stretching. The intermediate step between 2-D vorticity and 3-D turbulence is 3-D vorticity. This mechanism is presumed to be responsible for the high turbulence levels in the tube arrays. A two-dimensional simulation of the flow, therefore, contains no such mechanism for turbulence production. As a result, vorticity formed in the near wake is convected downstream and is destroyed upon impingement on a downstream tube. This is graphically illustrated in figure 7. The profile at x/d = 3.15 shows that a sharp peak in the r.m.s. velocity is predicted near y/d = -0.1, whereas in the experimental results no such peak is evident. This peak is caused by the passage of the vortices formed behind the tube in the first row. In the experiment, however, vorticity has dissipated into 3-D turbulence at this distance downstream. Inspection of the predicted time-series verified that the velocity fluctuations are mainly due to the variation of the mean flow associated with vortex shedding and that turbulent fluctuations appeared further downstream in the array (after row 3). Furthermore, a 2-D flow will tend to overestimate the velocity fluctuations associated with vortex shedding in the absence of a 3-D mechanism for the loss of vorticity. To take this point further, it is noted that the steady flow numerical predictions are in better agreement with the pulsating rather than the steady flow experimental results. A remarkable feature of the pulsating flow is that it produces an instantaneously two-dimensional flow; streamwise vortices disappeared at lock-on. Therefore, better agreement of the numerical results is obtained with the more 2-D pulsating flow. Recent predictions using the same model as the one used in the present study but in three dimensions show excellent agreement with the experimental results.

4 SUMMARY

The cross-flow over three tube arrays was examined by means of LDA measurements and flow visualisation. Numerical solutions of the flow were obtained using the Smagorinsky sub-grid scale model in two dimensions. It was found that the arrangement of the tubes exerts a strong influence on the vortex shedding characteristics in steady flow. Pulsing the flow resulted in lock-on in all arrays when the pulsation frequency was close to the frequency of unforced vortex shedding or its first harmonic but resonance was more pronounced in the latter case. Modification of the vortex shedding characteristics was accompanied by changes in the mean and r.m.s. velocities. The amplitude of the velocity fluctuations increased with lock-on due to an increase of the organised periodic motion of the flow associated with vortex shedding, whereas the level of random fluctuations remained approximately the same as in steady flow.

The numerical results agreed reasonably well with the experimental data if comparison is made with predictions based on standard turbulence models. The predicted trends for the effects of flow pulsation agreed with the experimental observations. Three-dimensional effects can account for the discrepancies between numerical and experimental results indicating that the limitation of the computational domain to two dimensions is severe.

Further experiments are required to investigate whether the modification of the vortex shedding characteristics with lock-on can be used for heat transfer augmentation.

5 REFERENCES

Balabani, S., Bergeles, G., Burry, D. and Yianneskis, M. (1994) "Velocity characteristics of the cross-flow over tube bundles", *7th Int. Symp. on Applications of Laser Techniques to Fluid Mechanics*, Lisbon, paper 39.3.

Balabani, S. and Yianneskis, M. (1996) "Turbulence scales and spectra in staggered tube bundle flows", *8th Int. Symp. on Applications of Laser Techniques to Fluid Mechanics*, Lisbon, paper 33.3.

Barbi, C., Favier, D.P., Maresca, C.A., Telionis, D.P. (1986) "Vortex shedding and lock-on of a circular-cylinder in oscillatory flow", *J Fluid Mech.*, **170**, 527-544.

Base, T.E., Patel, J.M., Valaitis, G.C. (1981) "Heat-transfer from cylinders in unsteady-flow", *Can J Chem Engng*, **59**, 247-250.

Bouris, D., Bergeles, G. (1999) "Two-dimensional time dependent simulation of the subcritical flow in a staggered tube bundle using a subgrid scale model", *Int. J. Heat and Fluid Flow*, **20**, 105-114.

Cheng, C.H., Chen, H.N., Aung, W. (1997) "Experimental study of the effect of transverse oscillation on convection heat transfer from a circular cylinder", *J Heat Transfer*, **119**, 474-482.

Gau, C., Wu, J.M., Liang, C.Y. (1999) "Heat transfer enhancement and vortex flow structure over a heated cylinder oscillating in the crossflow direction", *J Heat Transfer*, **121**, 789-795.

Griffin, O.M., Hall, M.S. (1991) "Vortex shedding lock-on and flow-control in bluff body wakes – review", *J Fluids Engng*, **113**, 526-537.

Halim, M. S. and Turner, J. T. (1986) "Measurements of cross flow development in a staggered tube bundle", *3rd Int. Symp. on Applications of Laser Techniques to Fluid Mechanics*, Lisbon, paper 21.7.

Konstantinidis, E., Castiglia, D., Balabani, S. and Yianneskis, M. (2000) "On the flow and vortex shedding characteristics of an in-line tube bundle in steady and pulsating cross-flow" paper accepted for publication in the *Chemical Engineering Research and Design* Trans. IChemE, Part A.

Laurence, D. and Rollet-Miet, P. (1998) "LES and RANSE of turbulent flow in tube bundles", *2nd Int. Conference on Turbulent Heat Transfer*, May 31-June 4, Manchester.

Lilly, D. (1967) "The Representation of Small Scale Turbulence in Numerical Simulation Experiments", *Proc. IBM Scientific Computing Symposium on Environmental Sciences*, Ed. H.H. Goldstine, 195-210.

Meyer, K. E. and Larsen, P. S. (1994) "LDA study of turbulent flow in a staggered tube bundle", *7th Int. Symp. on Applications of Laser Techniques to Fluid Mechanics*, Lisbon, paper 39.4.

Mouzakis, G. Bergeles, G. (1991) "Numerical prediction of turbulent flow over a two dimensional ridge", *Int. J Num. Methods in Fluids*, **12**, 287-296.

Nishimura, T., Itoh, H., Miyashita, H. (1993) "The influence of tube layout on flow and mass-transfer characteristics in tube banks in the transitional flow regime", *Int. J Heat Mass Transfer*, **36**, 553-563.

Oengören, A. and Ziada, S. (1998) "An in-depth study of vortex shedding, acoustic resonance and turbulent forces in normal triangle tube arrays", *J Fluids and Structures*, **12**, 717-758.

Paidoussis, M. P. (1983) "A review of flow-induced vibrations in reactors and reactor components", *Nuclear Engineering and Design*, **74**, 31-60.

Papadakis G. and Bergeles G(1995) "A locally modified second order upwind scheme for convection terms discretisation", *Int. J Num. Methods for Heat and Fluid Flow*, **5**, 49-62.

Patankar, S. V. and Spalding D. B. (1972) "A calculation procedure for heat, mass and momentum transfer in three dimensional parabolic flows", *Int. J Heat Mass Transfer*, **15**, 1787-.

Polak, D.R., Weaver, D.S. (1995) "Vortex shedding in normal triangular tube arrays", *J Fluids and Structures*, **9**, 1-17.

Price, S.J., Paidoussis, M.P., Mark, B. (1995) "Flow visualization of the interstitial cross-flow through parallel triangular and rotated square arrays of cylinders ", *J Sound Vib*, **181**, 85-98.

Rhie, C. and Chow, W. (1983) "Numerical study of the turbulent flow past an airfoil with trailing edge separation", *AIAA Journal*, **21**, 1525-1532.

Scholten, J. W., Murray, D. B. and Fitzpatrick, J. A. (1996) "Measurements of unsteady velocity and heat transfer for cylinders in cross-flow", *8th Int. Symp. on Applications of Laser Techniques to Fluid Mechanics*, Lisbon, paper 33.1.

Schumann U. (1975) "Subgrid scale model for finite difference simulations of turbulent flows in plane channels and annuli", *J. Computational Physics*, **18**, 376-404.

Simonin, O. and Barcouda, M. (1986) "Measurements of fully developed turbulent flow across tube bundle", *3rd Int. Symp. on Applications of Laser Techniques to Fluid Mechanics*, Lisbon, paper 21.5.

Simonin, O. and Barcouda , M. (1988) "Measurements and prediction of turbulent flow entering a staggered tube bundle", *4th Int. Symp. on Applications of Laser Techniques to Fluid Mechanics*, Lisbon, paper 5.23.

Smagorinsky, J. (1963) "General circulation experiments with the primitive equations. I. The basic experiment", *Monthly Weather Review*, **91**, 99-164.

Sung, H.J., Hwang, K.S., Hyun, J.M. (1994) "Experimental-study on mass-transfer from a circular-cylinder in pulsating flow", *Int. J Heat Mass Transfer*, **37**, 2203-2210.

Telionis, D.P., Gundappa, M., Diller, T.E. (1992) "On the organization of flow and heat-transfer in the near wake of a circular-cylinder in steady and pulsed flow", *J Fluids Engng*, **114**, 348-355.

Weaver, D.S. and Fitzpatrick, J.A. (1988) "A review of the cross-flow induced vibrations in heat exchanger tube arrays", *J Fluids and Structures*, **2**, 73-93.

Weaver, D.S., Fitzpatrick, J.A. and Elkashlan, M. (1987) "Strouhal numbers for heat-exchanger tube arrays in cross flow", *J Pressure Vessel Tech*, **109**, 219-223.